INTERNATIONAL ATOMIC ENERGY AGENCY
UNITED NATIONS EDUCATIONAL, SCIENTIFIC AND CULTURAL ORGANIZATION
INTERNATIONAL CENTRE FOR THEORETICAL PHYSICS
I.C.T.P., P.O. BOX 586, 34100 TRIESTE, ITALY, CABLE: CENTRATOM TRIESTE

H4.SMR/453-16

TRAINING COLLEGE ON PHYSICS AND CHARACTERIZATION OF LASERS AND OPTICAL FIBRES

(5 February - 2 March 1990)

Xe-CI DISCHARGE DIAGNOSTIC BY HOLOGRAPHIC INTERFEROMETRY

T. Letardi

ENEA
Centro Ricerche Energia
Roma, Frascati 00044
Italy

ISSN/0393-6333

ENEA
COMITATO NAZIONALE PER LA RICERCA E PER LO SVILUPPO
DELL'ENERGIA NUCLEARE E DELLE ENERGIE ALTERNATIVE

XeCl DISCHARGE DIAGNOSTIC BY HOLOGRAPHIC INTERFEROMETRY

A. DE ANGELIS, P. DI LAZZARO, F. GAROSI, G. GIORDANO, T. LETARDI
ENEA - Dipartimento Tecnologie Intersettoriali di Base, Centro ricerche energia Frascati

RT/TIB/87/51

Testo pervenuto nel febbraio 1988
Progetto Enea: Tecnologie ottiche ed elettro-ottiche (QU)

Summary

A direct measurement of the electron density time evolution in the active medium of a self-sustained XeCl laser discharge has been performed by means of the holographic interferometry technique. The time and space resolved behaviour of the discharge seems to confirm that the halogen depletion instability and the hot spots developing in the cathode region are the basic mechanisms which determine the premature termination of the output laser pulse.

Riassunto

L'evoluzione temporale della densità elettronica nel mezzo attivo di un laser a XeCl pompato con scarica autosostenuta è stata ottenuta (misurata) tramite la tecnica di interferometria olografica. I risultati delle misure risolte sia spazialmente che temporalmente hanno permesso di individuare lo sviluppo dei "punti caldi" nella regione catodica e l'instabilità del consumo della componente alogena del mezzo attivo quali fattori determinati nella fine prematura dell'impulso laser.

1. INTRODUCTION

Discharge pumped excimer lasers provide reliable and low maintenance sources of powerful ultraviolet radiation for wide industrial and medical applications. Despite the central role played by the plasma chemistry in the optimization of such a kind of laser system, it still remains a controversial field of investigation for chemists and physicists. Due to the varied nature and the complexity of the processes occurring in a laser gas mixture under the pumping excitation and ultraviolet radiation, the macroscopic information provided by most of the excimer literature (e.g., discharge current and voltage, laser gain and pulses) is insufficient to explain the observed laser characteristics.

A very restricted number of time resolved diagnostics has been published and the electron density evolution in a discharge pumped XeCl laser has been measured for the first time only recently.[1,2] In particular, the interferometric analysis of the refractive index[1,3] seems to be a more suitable diagnostic method for the measurement of electron density in a pulsed laser discharge than other optical methods, such as the Stark broadening of the $H\beta$ line[2] or the bremsstrahlung and line radiation.[4] This is because of the reliability, the achievable accuracy and the invaluable quantitative and pictorial diagnosis provided by the interferometric technique.

In this letter we present some holographic interferometric measurements of the discharge of a high uniformity, X-ray preionized, self-sustained discharge XeCl laser realized at the ENEA Center of Frascati, in the frame of a RGH laser development program.[5]

The temporal and spatial evolution of the electron density and a direct evaluation of the cathode filament growth rate have been obtained with good accuracy, allowing a deeper insight into the topical problem of the premature termination of lasing before the end of power deposition in self-sustained excimer lasers.[6,7]

2. SENSITIVITY AND ACCURACY OF THE METHOD

The refractivity of a plasma is given by

$$(n-1) = (n_e-1) + \Sigma_k(n_k-1) \qquad (1)$$

where (n_e-1) and (n_k-1) are the components due to the electron density N_e and to the heavy particle density N_k, respectively. If the radiation frequency is much higher than the plasma frequency and far enough from the resonance frequencies of the heavy particles, Eq. (1) may be approximated by[3]

$$(n-1) = \Sigma_k(A_k+B_k/\lambda^2)N_k - 4.47\cdot10^{-14}N_e\lambda^2 \qquad (2)$$

where A_k and B_k are characteristic coefficients of the species considered and λ is the radiation wavelength in cm.

In interferometric measurements of the refractivity of a homogeneous plasma layer of thickness L, the normalized fringe shift S caused by introducing an optical path difference is related to the refractivity variation $\Delta(n-1)$ by the expression

$$S = \frac{L}{\lambda}\Delta(n-1) \qquad (3)$$

Usually, $\Delta(n-1)$ refers to the initial state characterized by $N_e=0$. Therefore, from Eqs. (2) and (3) we have

$$S = L[\Sigma_k(A_k/\lambda+B_k/\lambda^3)\overline{\Delta N_k} - 4.47\cdot10^{-14}N_e\lambda] \qquad (4)$$

where $\overline{N_e}$ and $\overline{\Delta N_k}$ are the electron density and the heavy particle density variation averaged on the plasma thickness L. In the visible spectral region, the contribution of the heavy particles to the fringe shift is negligible (under opportune conditions as discussed below) compared to the electronic contribution.[3,8] In this case, expression (4) can be simplified as follows:

$$S = -4.47\cdot10^{-14}\overline{N_e}\lambda L \qquad (5)$$

The predominant heavy particle species in our XeCl gas mixture is the buffer gas Ne. Then, the previous assumption implies that

$$\frac{\overline{\Delta N_{Neon}}}{\overline{N_e}} << \frac{4.47\cdot10^{-14}\lambda}{A/\lambda + B/\lambda^3} \approx 90$$

after using the A and B values for Ne at λ=694 nm reported in Ref. 9. The reader is referred to the first paper of Ref. 3 for a detailed discussion on this point.

The sensitivity limit of the electron density measurement can be evaluated assuming for the smallest detectable

fringe shift the realistic value S=0,1. From Eq.(5) we have $(N_e L)_{min} \simeq 3.2\ 10^{16}\ cm^{-2}$.

3. EXPERIMENTAL

The X-ray preionized, self-sustained discharge XeCl laser investigated has been described in detail in previous papers[5]. Thus we report here just the main characteristics: The laser system consists of a 1-liter active volume cell (dimensions 3.5x4x80 cm^3) operating with a gas mixture (HCl:Xe:Ne) = (1:6.7:2019) at a total pressure of 4 atm. The best performances obtained maximizing the efficiency ϵ or the laser output energy E_L are summarized in Table 1. Laser pulses of more than 20 MW (>3 J in 150 ns) at 308 nm have been obtained, with a uniformity better than 90% in a 3.5x3.5 cm^2 laser spot and 2 mrad full angle divergence.

Throughout all the measurements reported here, the excitation rate was kept constant at the value W = 290 kW/cm^3.

Interferometric measurements of the electron density evolution of the outlined XeCl laser have been carried out using the holographic system depicted in Fig. 1. The laser source is a holographic JK 2000 ruby laser, which can deliver a double pulse with more than 1 m coherence length. Each pulse has a 5-J energy and a 20-ns FWHM duration. The delay time between the pulses may be settled in the range 1:800 μs.

With the double pulse operation, temporal aberrations as well as problems related to the "laser snow" effect can be avoided.[10]

TABLE 1

Best Performances of XeCl Laser

Max output laser energy E_L	Max efficiency ϵ
E_L = 3.2 J	E_L = 1.5 J
$\epsilon_{intrinsic}$ = 2.6%	$\epsilon_{intrinsic}$ = 3.6%
ϵ_{plug} = 0.7%	ϵ_{plug} = 2%
Excitation rate = 850 kW/cm^3	Excitation rate = 190 kW/cm^3

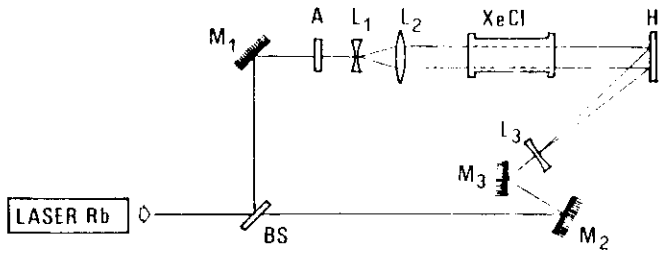

Fig.1 Experimental setup employed in the holographic interferometry measurements of the time evolution of the XeCl discharge plasma. B.S. is a beam splitter with reflectivity r=95%; M_1 and M_3 are totally reflecting flat mirrors; A is an attenuator; the lens system L_1-L_2 acts as a beam expander; M_3 is a vibrating mirror; L_3 is a lens with focal length f=-8 cm; H is a Kodak holographic film plate.

Referring to Fig. 1, the attenuator A allows a correct intensity balance between the object and the reference beam; the rotating mirror M_2 is synchronized to the ruby laser allowing the change in the reference beam direction during the interval between exposures. This leads to the appearance of a reference fringe pattern in the reconstructed holographic interferograms.[8] A distinct optical circuit using a scatterer plate instead of the beam expander L_1-L_2 (see Fig. 1) has also been realized. This setup could be relevant to the observation of phenomena (e.g., arcs, hot spots) localized at different points along the XeCl optical axis.

4. RESULTS

The ability to probe the active medium of the XeCl laser at different times after the discharge breakdown using the described setup made it possible to study the spatial and temporal behaviour of the discharge plasma.

Some typical holograms obtained at different delays are shown in Fig. 2 where the development and the diffusion of streamers from the cathode region are evident. A possible explanation of the rise of this phenomenon after a short delay time (Fig.2a) is that the electron drift away from the cathode leaves a depleted region where the electron density falls down the critical value to generate the filamentation.[11] In our case, however, the discharge voltage risetime of about 25 ns should be short enough to avoid a substantial electron depletion in the cathode sheath.

An alternative explanation is the cathode layer instability phenomenon[12]: a random increase in the current enhances the ion density in the cathode layer increasing the cathode field and allowing the field-emission current to grow further. This leads to formation of a cathode spot with a growth time in the ns region.[12,13] In our case, the initial spatial inhomogeneity of the electric field (with local instantaneous values of $E \gtrsim 10^6$ V/cm)[12] could be originated from the perforated screen cathode structure.[5]

Anyhow, the effect of the filament propagation becomes dramatic as the time progresses (Fig. 2b, 2c) because of the dissociative attachment and other processes (e.g. the ambipolar drift fluxes of plasma) which contribute to the rapid growth of the discharge instabilities.[7,14]

A pinching effect of the discharge width in the anode region is clearly visible in Fig. 2c.

The discharge collapse is fully developed 600 ns after the discharge breakdown (Fig. 2d), and the filaments bridge the electrode gap without an arc occurring.

The measurement set has been repeated filling the laser cell with pure Ne. The results showed that the discharge instabilities arise slower and in a less dramatic manner with respect to the normal laser gas mixture, confirming the main role played by HCl and Xe in the discharge deterioration.[6,7]

A visual inspection of the holograms obtained using a scatterer at the input of the XeCl laser cell in the interferometer schematized in Fig. 1 confirmed the presence of several hot spots, distributed in the perforated cathode area.

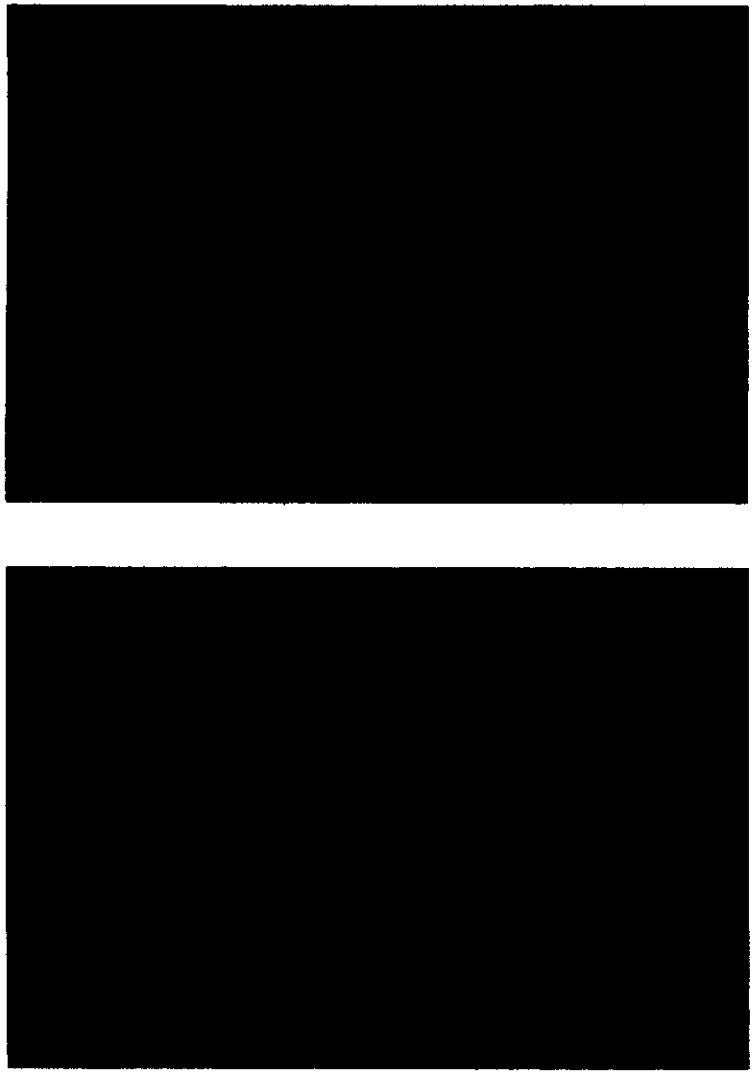

Fig.2 Typical interferograms of the XeCl active medium with an electrode separation of 4 cm. Delay time since the discharge breakdown: a) 135 ns; b) 215 ns; c) 350 ns; d) 615 ns.

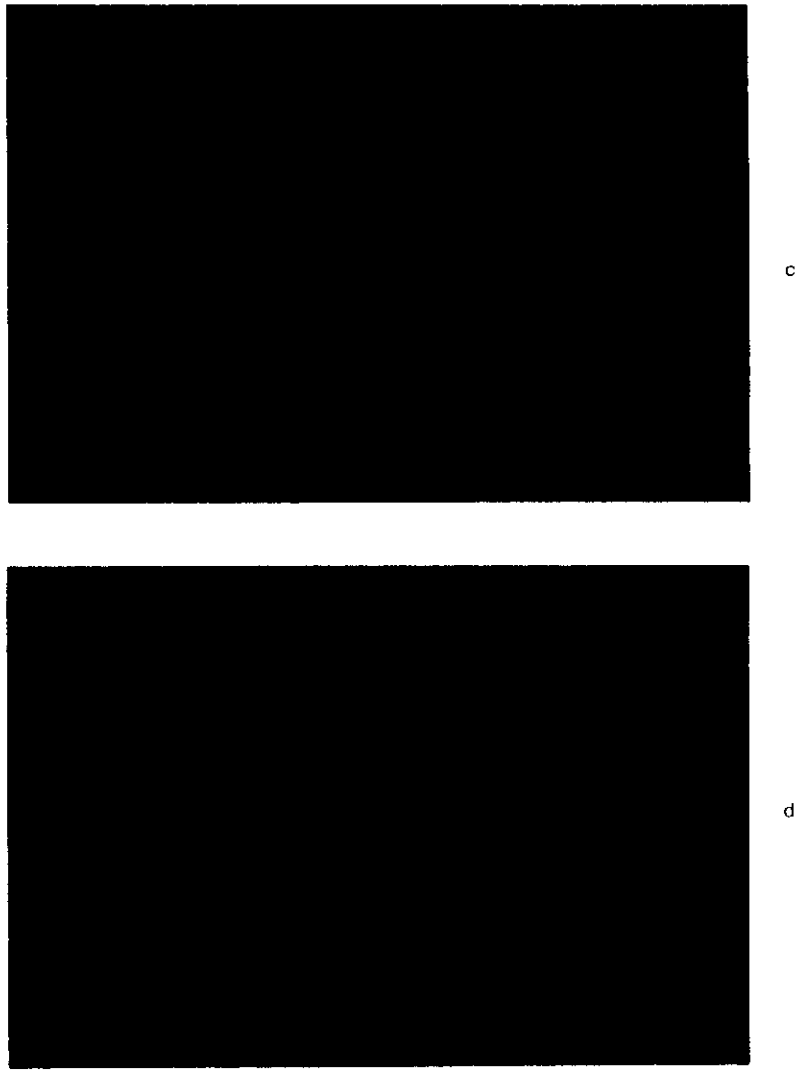

Fig.2 Typical interferograms of the XeCl active medium with an electrode separation of 4 cm. Delay time since the discharge breakdown: a) 135 ns; b) 215 ns; c) 350 ns; d) 615 ns.

The time dependence of the cathode filament growth is reported in Fig. 3 from which we can deduce an initial growth rate of $V_F=(3.7\pm0.3)$ cm/μsec considering the data below the 200 ns delay range. This value is about a factor two higher than the published electron drift velocity estimated values for Ne-based XeCl gas mixes[1,5,6] confirming that distinct effects contribute to the filament generation and growth.[13,14]

Figure 4 shows the interferometrically determined electron density as a function of time. The discharge current and the laser output waveforms are also indicated. The reported electron density data have been calculated by means of an elaboration of the holographic interferograms using an image analysis system. In this way a very careful determination of both the peak and the spatially averaged fringe inflection has been obtained.

A large electron density (up to $3\cdot10^{15}$ cm^{-3}) is generated in the transient glow discharge, the maximum occurring ~100 nsec delayed against the current maximum. The relatively slow electron density decay after 400 ns is consistent with the experimental waveform of the current damped oscillations which result (in this delay region) more stressed than the simulated ones obtained using an exponentially decreasing discharge resistance parametrization.[5]

5. COMMENTS

The experimental results on the temporal and spatial evolution of the XeCl discharge reported in the previous section seem to confirm some important observations pointed out in Ref. 6: in the initial stage of the discharge, hot

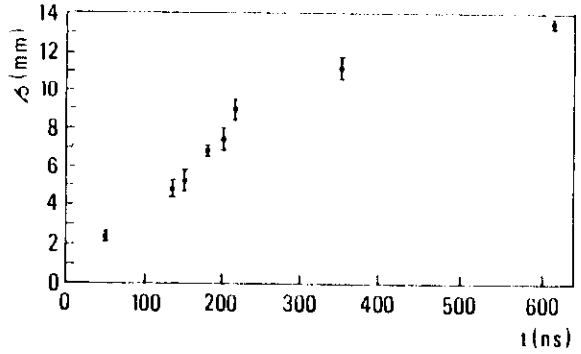

Fig.3 Cathode filament growth versus the delay with respect to the discharge voltage breakdown.

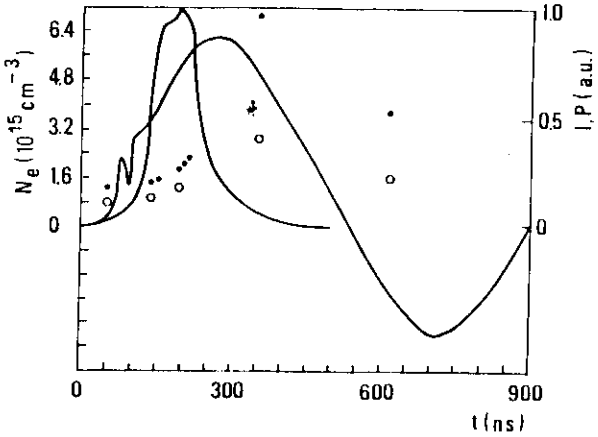

Fig.4 Electron density time history obtained from the interferograms elaborated by an image analysis system. The open and the full dots indicate the spatially averaged and the peak values of the electron density, respectively. The laser pulse and the discharge current are also reported.

spots do develop at the cathode,[13] and the halogen gas in the mix promotes the initial growth of a well defined filament from each hot spot. Filament development leads to glow discharge collapse, and although electrical power can still be deposited into the discharge in a fully developed filamentary mode without arcing, strong induced discharge inhomogeneities lead to premature lasing disruption.

Concerning the local depletion of the halogen donor model to explain the mechanism of the discharge filamentation, the theory presented in Ref. 7 indicates that in the early stages of the discharge, $N_e(t)$ grows according to an expression whose lowest order terms are

$$N_e(t) \sim N_e(0)\left[1 + \frac{k^2 N_e(0) t^2}{2} [HCl]_0 + \ldots\right] \qquad (6)$$

where $N_e(0)$ and $[HCl]_0$ are the electron number density and halogen donor concentrations at the inception of the discharge, and k is the effective electron dissociative attachment rate. We compared the relationship (6) with our experimental electron density time evolution and guessed values of the rate coefficient k. The result is reported in Fig. 5. The agreement is good in the range below the 300-ns delay time. At later times, the electron density grows faster due to the effect of the higher order terms in Eq.(6).

The $k=10^{-9}$ cm^3/s rate value used plotting Eq.(6) was the effective one for attachment to vibrationally excited HCl, according to Refs. 15 and 16. Besides, it is only a factor two lower than a recently estimated k value obtained by

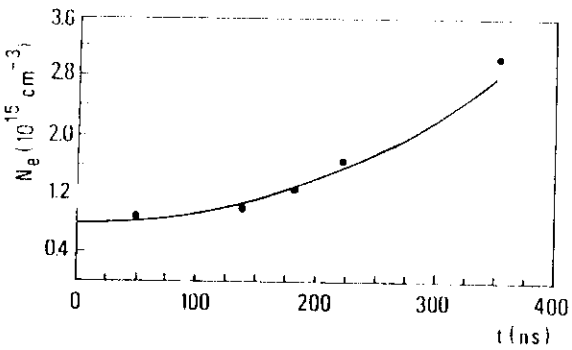

Fig.5 Electron number density growth as results from Eq. (6) (continuous line) and from our experimental data (dots). $[HCl]_0 = 4.9 \cdot 10^{16}$ cm^{-3}; $k = 10^{-9}$ $cm^3 s^{-1}$.

means of the emission from high lying ionic states of a discharge XeCl laser driven by a PFL, working with a different excitation rate and gas mixture composition.[17]

Let us devote a final comment to the use of a perforated screen cathode instead of a flat one. There is a lot of experimental evidence that even small cathode surface irregularities may actually promote discharge filamentation.[12,13,18] In Ref.6 Taylor estimated the sensitivity of the final discharge electron density to small change of the electric field. He showed that a small local $\Delta E/E \sim 0.2\%$ produces a substantial $\Delta N_e/N_e \sim 8\%$ and drew the conclusion that the electrode profile is a critical factor in determining the uniformity of the discharge. However, in our experience, the perforated screen cathode offers some practical advantages to the overall performances of the laser output energy and uniformity, according to Ref.19.

The very large number of critical parameters in an excimer laser discharge (e.g., the preionization electron number density, the rise time of the discharge voltage and current, the d.c. breakdown level of the gas mixture, the net optical gain, and so on) makes it sometimes difficult to compare different laser systems and generalize some experimental results.

Certainly, this is one of the points which needs further experimental investigation.

REFERENCES

1. J.E. Ford, J. Meyer, H. Boutman, Appl. Phys. Lett. 48, 1639 (1986).
2. R.C. Hollins, D.L. Jordan, J. Coutts, J. Phys. D; Appl. Phys. 19, 37 (1986); M. Hiramatsu, H. Furuhashi, T. Goto, J. Appl. Phys. 60, 1946 (1986).
3. S. Martellucci: Supplemento al Nuovo Cimento 5, 642 (1967); W. Ross, J. Phys. D: Appl. Phys. 13, 1371 (1980); A.N. Zaidel, Sov. Phys. Usp. 29, 447 (1986).
4. Yu. B. Golubovskii, V.V. Kulivov, Opt. Spectros. (USSR) 60, 707 (1986).
5. A. De Angelis, E. Fiorentino, G. Giordano, T. Letardi, E. Sabia, M. Vannini, "High uniformity X-ray preionization discharge XeCl laser" in Proc. of Int. Conf. on Lasers '84, Eds. K.M. Corcoran, D.M.Sullivan, W. C. Stwalley, (STS Press, McLean VA 1985) p.606; T. Letardi, S. Bollanti, A. De Angelis, P. Di Lazzaro, I. Gabbai, G. Giordano, E. Sabia, "Characterization of a high uniformity, X-ray preionized XeCl laser", to be published in Nuovo Cimento D.
6. R.S. Taylor, Appl. Phys. B 41, 1 (1986).
7. J. Coutts, C.E. Webb, J. Appl. Phys. 59, 704 (1986).
8. G.V. Ostrovskaya, Yu. I. Ostrovsky, "Holographic methods of plasma diagnostic" in Progress in Optics XXII, Ed. E. Wolf (Elsevier, Amsterdam, 1985) p. 199.
9. U. Ascoli Bartoli, "Plasma diagnostics based on refractivity" in Plasma Physics, Ed. A. Hamende (Vienna, 1965) p. 287.
10. N. Beverini, K. Ernst, N. Inguscio, F. Strumia, Appl. Phys. B 26, 57 (1981); V.I. Donin, Yu. I. Khapov,

Sov. J. Quantum Electron. 16, 1034 (1986).

11. J. Levatter, S. Lin, J. Appl. Phys. 51, 210 (1980).
12. G.A. Mesyats, Sov. Tech. Phys. Lett. 1, 385 (1975); G.A. Mesyats, Sov. Tech. Phys. Lett. 1, 292 (1975).
13. G.A. Mesyats, Yu. D. Korolev, Sov. Phys. Usp 29, 57 (1986).
14. F.I. Vysikailo, Sov. J. Plasma Phys. 13, 122 (1987).
15. E. W. McDaniel and W.L. Nighan Eds., "Applied Atomic Collision Physics" (Academic, N.Y., 1982) Vol. 3, pp. 61-65, pp. 325-328.
16. J.K. Ku, D.W. Setser, Appl. Phys. Lett. 48, 689 (1986).
17. M.R. Osborne, private communication.
18. L.J. Denes, W.R. Goss, I.E. Kanter, L.E. Kline, Bull. Am. Phys. Soc. 25, 109 (1980); P. Suleebka, M.R. Barrault, J.D. Craggs, J. Phys. D 8, 2190 (1975); Yu. D. Korolev, V.A. Kusmin, G.A. Mesyats, Sov. J. Plasma Physics 8, 708 (1982).
19. K. Midorikawa, M. Obara, T. Fujioka, IEEE J. Quantum Electron. QE-20, 198 (1984).

Edito dall'ENEA Direzione Centrale Relazioni
Viale Regina Margherita 125 Roma
Finito di stampare in settembre 1988

Fotoriproduzione e stampa
a cura della Arti Grafiche S. Marcello